Thin-Walled Structures 107 (2016) 453–461

Contents lists available at ScienceDirect

Thin-Walled Structures

journal homepage: www.elsevier.com/locate/tws

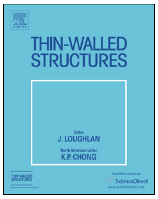

Full length article

Composite action of octagonal concrete-filled steel tubular stub columns under axial loading

Fa-xing Ding [a], Zhe Li [a,*], Shanshan Cheng [b], Zhi-wu Yu [a,c]

[a] School of Civil Engineering, Central South University, Changsha 410075, PR China
[b] Department of Civil and Structural Engineering, University of Sheffield, United Kingdom
[c] National Engineering Laboratory for High Speed Railway Construction, Changsha 410075, PR China

ARTICLE INFO

Article history:
Received 3 April 2016
Received in revised form
11 July 2016
Accepted 15 July 2016
Available online 25 August 2016

Keywords:
Octagon
Composite action
Ultimate bearing capacity
Practical formula
Strain ratio
Confinement coefficient

ABSTRACT

This paper presents a combined experimental, numerical and theoretical study on the mechanical performances of octagonal CFT stub columns subjected to axial compressive loading. Eight specimens of axial compression tests have been carried out aiming at investigating the effects of the concrete strength and steel ratio on the mechanical and deformed behavior of octagonal CFT stub columns. 3D finite element modelling was established for parametric studies to probe into the composite action between the steel tube and the core concrete of the octagonal CFT stub column. In addition, a practical formula has been proposed to predict the ultimate bearing capacity of the octagonal CFT stub column with the confinement coefficient of 1.5, which is an amplification coefficient of the vertical bearing capacity of steel tube considering the composite action between the core concrete and the steel tube.

1. Introduction

A concrete-filled steel tube (CFT) column is a composite member which is consisted of a steel tube filled with concrete. The concrete core adds stiffness to the steel tube and prevents the occurrence of inward local buckling, while the steel tube improves the compressive strength and deformed performance of the core concrete. Given the favorable actions such as high strength, high ductility and large energy absorption capacity, the CFT column has been widely used in practical structures especially in long-span, high-rise and heavy-sustainment structures [1].

The large aggregation of experimental and numerical studies on CFT columns with circular and square cross-sections used in common under the axial compressive load has been conducted in literature [2–10]. Mechanical behavior of the circular [11], square [12] and rectangular-with-round-ends [13] sectional CFT stub columns under axial loading have been investigated by the co-author Ding, and practical formulas of load-bearing capacities have been proposed with the corresponding confinement coefficient.

However, available studies on octagonal CFT stub columns are rather few in literature, although octagonal cross-sections are demanded in architectural design in some cases. Experimental studies on octagonal CFT stub columns has been conducted by Tomii [14]. Yu [15] presented a unified formula of the ultimate load-bearing capacity for circular and polygonal CFT columns subjected to axial compression.

Eight axial compression specimens of octagonal CFT stub columns have been conducted at the Central South University in China to investigate the composite action between the core concrete and the steel tube of octagonal CFT stub columns. The nonlinear finite element analysis (FE) of octagonal CFT stub columns throughout loading history has been carried out using the commercial software ABAQUS. Based on the above FE results, the strain ratio of steel tube and the stress distribution of core concrete and steel tube at the corner and mid-points have been illustrated, as well as the practical formulas for the ultimate bearing capacity of octagonal CFT stub columns have been proposed by using superposition principle at the ultimate state and simplification on stress contour, which follows the same research idea as Ding et al. [11–13]. Details of the studies have been explained in the following sections of this paper.

2. Experimental investigation

2.1. Materials

Two types of concretes were applied with cubic compressive strengths 39.3 MPa and 57.4 MPa respectively, at a curing age of 3 months. The cubic compressive strength and elastic module of

---

[*] Corresponding author.
E-mail address: 09lizhe@163.com (Z. Li).

http://dx.doi.org/10.1016/j.tws.2016.07.012
0263-8231/

Nomenclature

A_c	Cross-sectional area of core concrete ($=A_{c1}+A_{c2}=2b^2\tan 67.5°$)
A_{c1}	Unconstrained area of core concrete ($=0.3A_c$)
A_{c2}	Constrained area of core concrete ($=0.7A_c$)
A_s	Cross-sectional area of steel tube ($=8bt$)
A_{sc}	Total area of cross-section ($=A_s+A_c$)
B	Edge length of octagonal section
b	Edge length of core concrete ($=B2t\tan 22.5°$)
DI	Ductility index, given by $DI=\varepsilon_{0.85}/\varepsilon_b$, where $\varepsilon_b=\varepsilon_{0.75}/0.75$
E_s	Elastic modulus of steel tube ($=2.06\times10^5$ MPa)
f_c	Compressive strength of prism volume
f_{cu}	Compressive strength of cubic concrete
f_{sc}	Ultimate strength of CFT columns
f_u	Ultimate strength of steel tube ($=1.5f_y$)
f_y	Yield strength of steel tube
k	Ratio of initial tangent modulus to secant modulus at peak stress
L	Height of specimens
N	Axial load
N_u	Ultimate bearing capacity
$N_{u,\ Eq.10}$	Ultimate bearing capacity of octagonal CFT stub columns from Eq. (10).
$N_{u,\ Exp}$	Ultimate bearing capacity of octagonal CFT stub columns from experimental results
$N_{u,\ FE}$	Ultimate bearing capacity of octagonal CFT stub columns from FE results
$N_{u,[15]}$	Ultimate bearing capacity of octagonal CFT stub columns from reference [15]
p	Lateral pressure coefficient
t	Wall thickness of steel tube
σ	Axial stress of concrete
σ_i	Equivalent stress of steel tube
$\sigma_{L,c}$	Axial compressive stress of core concrete
$\sigma_{L,s}$	Axial compressive stress of steel tube
$\sigma_{r,c}$	Radial compressive stress of constrained concrete
$\sigma_{\theta,s}$	Tensile transverse stress of steel tube
$\varepsilon_{0.75}$	Axial strain when the load attains 75% of the ultimate load in the pre-peak stage
$\varepsilon_{0.85}$	Axial strain when bearing capacity is decreased to 85% of ultimate value
ε	Axial strain of concrete
ε_c	Strain corresponding with the peak compressive stress of concrete
ε_L	Axial strain of CFT columns
$\varepsilon_{L,s}$	Axial compressive strain of steel tube
ε_i	Equivalent strain of steel tube
ε_y	Yield strain of steel tube
ε_{st}	Hardening strain of steel tube ($=12\varepsilon_y$)
ε_u	Ultimate strain of steel tube ($=120\varepsilon_y$)
$\varepsilon_{\theta,s}$	Tensile transverse stress of steel tube
ν_{sc}	Strain ratio of steel tube ($=\varepsilon_{\theta,s}/\varepsilon_{L,s}$)
ρ	Steel ratio of columns ($=A_s/A_{sc}$)

Table 1
Properties of steel.

Thickness	f_y (MPa)	f_u (MPa)	E_s (MPa)	ν_s
4 mm	311	460	2.09×10^5	0.292
6 mm	321	480	2.02×10^5	0.256

concrete were measured in accordance with the standard GB/T50081-2002 [16]. Moreover, two types of steel were adopted in the test, of which the material properties were determined through tensile coupon tests. Three coupons were cut and tested in accordance with the standard GB/50017-2003 [17]. The yield strength, ultimate tensile strength, elastic module and Poisson's ratio of steel were listed in Table 1.

2.2. *Test specimens*

A total of 4 groups of octagonal CFT were designed in this study and the details were shown in Table 2. Each test was repeated twice (namely A and B), and thereby eight specimens were made in total. The nominal dimensions of each specimen were 200 (B) mm × 4(6) (t) mm × 1500 (L) mm, where B is the outer edge length of the octagonal section, t is the wall thickness of the steel tube and L is the height of the specimen.

The octagonal steel tubes were molded by bending steel plates into grooves and then welding the two edges at the corner. The positions at which the butt welds were made were labelled in Fig. 1.

For a better observation of deformation and preventing steel tubes from rusting, red paint was sprayed on the outer surface of the steel tubes and grids of 50 mm × 50 mm were drawn on the

Table 2
Properties of specimens and comparison between calculated results and tested ones.

Reference	Specimens	$B\times t$ (mm)	L (mm)	f_{cu} (MPa)	f_y (MPa)	Steel ratio ρ	DI	$N_{u,\ Exp}$ (kN)	$N_{u,\ FE}$ (kN)	$N_{u,\ Eq.10}$ (kN)	$N_{u,[15]}$ (kN)	$N_{u,\ FE}/N_{u,\ Exp}$	$N_{u,\ Eq.10}/N_{u,\ Exp}$	$N_{u,[15]}/N_{u,\ Exp}$
Present paper	OST1-A	201 × 3.85	1500	39.3	311	0.032	6.806	9297	8942	10,290	8069	0.968	1.107	0.868
	OST1-B	199 × 3.98				0.033	3.052	9311	8850	10,199	8012	0.950	1.095	0.861
	OST2-A	200 × 6.02			321	0.049	7.987	10,502	10,128	11,796	9466	0.964	1.123	0.901
	OST2-B	197 × 5.89				0.049	7.734	10,713	9800	11,418	9160	0.915	1.066	0.855
	OST3-A	200 × 3.92		57.4	311	0.032	3.984	12,362	12,048	13,631	11,055	0.975	1.103	0.894
	OST3-B	199 × 4.02				0.033	4.034	12,357	11,906	13,572	11,015	0.964	1.098	0.891
	OST4-A	197 × 5.88			321	0.049	8.054	12,992	12,582	14,637	12,025	0.968	1.127	0.926
	OST4-B	198 × 5.98				0.049	5.312	13,263	12,787	14,832	12,189	0.964	1.118	0.919
Reference[14]	2HN	62.1 × 2.0	/	38.06	341.3	0.053	/	1003	968	1173	925	0.965	1.170	0.923
	3HN	62.1 × 3.2			300.2	0.084		1100	1133	1350	1084	1.030	1.227	0.986
	4HN	62.1 × 4.0			294.3	0.104		1273	1241	1489	1210	0.975	1.170	0.950
											Avg.	0.967	1.128	0.907
											St. dev.	0.005	0.044	0.058